THE DISTRIBUTION OF Ga IN Ga-PILLARED MONTMORILLONITES: A TRANSMISSION ELECTRON MICROSCOPY AND MICROANALYSIS STUDY

Loc Duong[1,2*], Thor Bostrom[1,2], Theo Kloprogge[1], and Ray Frost[1]

[1] Inorganic Materials Research Program, School of Physical and Chemical Sciences, Queensland University of Technology, GPO Box 2434, Brisbane, Qld 4001, Australia
[2] Analytical Electron Microscopy Facility, Queensland University of Technology, GPO Box 2434, Brisbane, Qld 4001, Australia
[*] Corresponding author: E-mail l.duong@qut.edu.au

Later published as :

Duong, Loc. V. and Bostrom, Thor and Kloprogge, Theo and Frost, Ray (2005) The Distribution Of Ga in Ga-Pillared Montmorillonites: A Transmission Electron Microscopy And Microanalysis Study. *Microporous and Mesoporous Materials* 82(1-2):165-172.

ABSTRACT

The distribution of Ga in the interlayer of montmorillonite pillared with a Ga_{13} polyoxocation complex has been studied by transmission electron microscopy, energy-dispersive X-ray microanalysis (EDX), X-ray mapping and powder X-ray diffraction in combination with N_2 adsorption-desorption. To view the clay layers by TEM, the pillared clay was embedded in Spurrs resin in a preferred orientation, and sectioned with an ultramicrotome perpendicular to the layers. Montmorillonites pillared with Al_{13} and $Al_{12}Ga$ complexes were also prepared for microanalysis in the TEM. The Ga X-ray peaks could be easily distinguished in the EDX spectra, allowing concentrations relative to other elements to be determined. Elemental X-ray maps for Ga, Si and Al in the Ga_{13} pillared clay cross-sections demonstrated that the Ga was homogeneously distributed throughout the crystal thickness. Comparison of the analytical data with that from the Al_{13} and $Al_{12}Ga$ pillared clays and the starting material suggested that an approximately constant amount of the intercalated species per amount of Si in the clay became incorporated into the structure in each case. Calculation of the formula for the Ga-pillared montmorillonite showed that 0.89 Ga is present per formula unit containing 8 (Si+Al), which is equivalent to 20 silicate rings, each consisting of 6 tetrahedra, for every Ga_{13} pillar. The actual dimension of the pillar, based results from the elemental analyses and XRD is 8.7Å and the mean distance between the pillars is 44.3Å, which is in good agreement with the average pore size of 39Å obtained by N_2 adsorption-desorption measurements. This study shows a new approach for obtaining more detailed information on the pillars in pillared clay by combining analytical data from X-ray microanalysis with measurements by XRD and N_2 adsorption-desorption.

Keywords: Ga_{13}, Montmorillonite, Pillared clay, Textural properties, Transmission Electron Microscopy

1. INTRODUCTION

Pillared montmorillonites are microporous materials, obtained by ion exchange of montmorillonites with highly charged metallic species followed by a calcination process, that in the last 25 years have been developed as a new class of catalysts [1-5]. Producing suitable pillared montmorillonites for catalytic applications requires detailed understanding of the structure of the starting clay, the pillaring agent, and the size, shape and location of the oxidic pillars in the final products. Although extensive research has been undertaken in the field of pillared clay structures [1, 6-8], the complete structure of pillared clays especially the location, structure and bonding to the clay layers of the oxide pillars is still unknown.

Montmorillonites pillared with different polyoxocations have been prepared and studied for many years [1]. Al_{13} montmorillonites are the most common pillared clays [9], mainly because the Al polyoxocation gives a large basal d-spacing and, together with the very similar $Al_{12}Ga$ pillared montmorillonites, are quite stable at high temperatures, up to about 750^{o}C. The structures of Al_{13} and Ga_{13} are very similar with both having a Keggin structure in which a central $Al^{IV}O_4$ or $Ga^{IV}O_4$ is surrounded by twelve Al^{VI} octahedra with water and hydroxyl groups [10-15] resulting in similar basal d-spacings in the final pillared clays.

Transmission electron microscopy (TEM) has provided the necessary spatial resolution for studying the microstructure of clays down to the lattice level, but has required specific sample preparation procedures to achieve this. A preparation method for studying smectite layers by TEM has been discussed by Kim *et al.* [16]. TEM together with energy-dispersive X-ray spectrometry (EDX) has allowed chemical analysis of small areas down to about 20 nm and X-ray mapping of regions of a few hundred nanometers. This combination of structural and chemical analysis in the TEM is a powerful tool for studying complex, fine-grained clay minerals, and in particular pillared clays. However the achievable analytical spatial resolution may be limited by the electron beam sensitivity of some specimens. Ma *et al.* [17] used EDX in a TEM to study the loss of certain elements from a clay structure. The diffusion of alkali elements and higher atomic number elements (Fe, Ti) from clay minerals was found to be associated with crystal habit and instrumentation conditions. More specimen damage due to the electron beam was seen when the crystals were viewed in the plane perpendicular to the (001) direction than in the plane parallel to (001). The loss of elements may be reduced by using a lower beam current and a larger analysis area [17]. Crozier *et al.* [18] used analytical electron microscopy to confirm the location of Zr pillars in Zr-pillared montmorillonite. The Zr pillars were found to have an irregular shape and distribution in the silicate layers [18].

Montmorillonite pillared with Ga_{13} has some advantages over that pillared with Al_{13} for analytical TEM studies. As Ga has a higher atomic number (31) than Al, the intercalated Ga may potentially improve contrast in TEM images. Further, the element can be clearly detected by X-ray microanalysis without confusion with the Al in the clay structure. For comparative studies Al_{13} and $Al_{12}Ga$ pillared clays were also prepared. The pillared

montmorillonites were examined and analysed in the TEM mainly in cross-section, in other words with the c-axis oriented perpendicular to the electron beam. In this paper the results from transmission electron microscopy, EDX microanalysis, powder X-ray diffraction and N_2 adsorption-desorption measurements have been used to deduce the distribution of Ga in the structure of Ga_{13} pillared montmorillonite. It is shown that an approximately constant proportion of the intercalated species is incorporated into the clay structure in pillaring, and it is possible to calculate an average size and distribution of the pillars.

2. MATERIALS AND METHODS

2.1 Starting materials

The starting materials used for this study were $\leq$ 2 μm fractions of Wyoming montmorillonite SWy-2, and Miles montmorillonite from Queensland, Australia. The Miles montmorillonite has a significantly higher CEC than Swy-2. All samples were saturated with sodium through exchange with 1 M NaCl for 8 hours. The clays were washed five times with deionised water in order to remove residues of NaCl. A detailed description of the Miles material and the Al_{13}-pillaring procedure have been provided by Kloprogge *et al*. [19]. Miles montmorillonite was used to prepare the Al_{13} and $Al_{12}Ga$ pillared clays and SWy-2 montmorillonite was used to prepare the Ga_{13} pillared clay. The preparation of the $Al_{12}Ga$ and Ga_{13}-pillared clays was analogues to that of the Al_{13}-pillared clay. A 0.1M solution of NaOH was added to $Ga(NO_3)_3$ at a rate of 0.01 ml/min using a peristaltic pump under vigorous stirring at room temperature. The OH/Ga ratio was 2:1. The Al_{13}, $Al_{12}Ga$ and Ga_{13} solutions were added to the aqueous clay suspensions under continuous stirring for a period of four hours. The suspensions were then allowed to stand for several days. The pillared clays were washed 5 times with deionised water using a centrifuge. The samples were allowed to dry in air at ambient temperature. Finally, the samples were heated at 2°C/min and calcined at 450°C for 8 hours.

2.2. X-ray diffraction

X-ray diffraction (XRD) was used to check for the intercalation process of Ga into the clay structure before and after calcination by observing the changes in the (001) spacings. For powder XRD, the sample was ground and mixed with ethanol, deposited on a low background plate and dried at room temperature. Preferential orientation of the clay platelets is very common under these conditions, thus enhancing the (00l) reflections relative to other reflections. XRD patterns were collected using a PANalytical X'Pert Pro diffractometer with a rotating anode source and a diffracted beam curved graphite monochromator and CuKα radiation. Scans were made using a 0.05° step size at 0.5sec/step.

2.3 Sample preparation for Transmission Electron Microscopy

Smectites, due to their ability to absorb and desorb water and exchange cations, are very sensitive to the method used to prepare them for examination in the TEM and therefore care must be taken not to introduce preparation artefacts. For viewing the clay particles mainly parallel to the c-axis, a dilute suspension of montmorillonite in 70% alcohol was briefly ultrasonicated and a small drop of the suspension was placed on a thin carbon film

on a TEM copper grid, allowed to dry and coated with a thin carbon layer to improve stability under the beam.

In order to observe the clay in a direction perpendicular to the c-axis so that the layers could be viewed in cross-section, the clay was embedded in Spurrs resin [20] for ultramicrotoming. The morphology, swelling properties, water absorption, and reaction with the resin have to be taken into account when preparing smectite samples for TEM. Because of its low viscosity, Spurrs has long been used as an embedding agent for biological and material samples for electron microscopy, and was used here to obtain good penetration into the clay material. However the resin is intolerant of moisture in the sample, and therefore the samples had to be adequately dried before embedding. Figure 1 shows the steps used in the preparation of cross-sections of the pillared clays. Pillared montmorillonite was diluted with water and allowed to settle for about one week. The water was removed leaving the clay particles preferentially aligned with the bottom of the container. The sample was dried at 60-100^{o}C for two weeks before addition of the resin. After polymerisation overnight at 60^{o}C, the small resin plug was removed from the base of the container, rotated 90° and sectioned with a diamond knife using a Reichert ultramicrotome to produce cross-sections of the embedded particles. The sections were 60-80 nm in thickness. The starting montmorillonites were also prepared for microanalysis, but as these materials had not been calcined they was first dehydrated with alcohol and acetone to remove any residual water before impregnation with Spurrs resin.

2.4 Transmission Electron Microscopy

Specimens were examined in a Philips CM200 transmission electron microscope fitted with a LaB_6 cathode and operated at 200kV. For measurements of lattice spacings and electron diffraction patterns, TEM negatives were scanned at 600 or 1200dpi and measurements carried out on the digital images using image analysis software. Energy-dispersive X-ray microanalysis and X-ray mapping was carried out mainly in scanning transmission (STEM) mode using a Link thin-window X-ray detector and Link ISIS 300 microanalysis system (Oxford Instruments, UK). Quantitative calculations of element concentrations and atomic ratios were carried out using a thin-film matrix correction procedure, in which the total concentrations are normalised to 100%. For these calculations, the density of the material was taken as 3.0 g.cm^{-3} and the specimen thickness for each analysis was estimated from STEM images and the Si X-ray intensity.

2.5 Nitrogen adsorption-desorption

The surface areas of the starting montmorillonite and Ga_{13} pillared montmorillonite were calculated by the BET method using N_2 adsorption-desorption on a Micromeritics ASAP 2010 at a partial pressure range of 0.06 to 0.30. The pore size distribution and pore volume were calculated using the Tristar software.

3. RESULTS AND DISCUSSION

X-ray powder diffraction (XRD) patterns of the starting montmorillonite and Ga_{13} pillared montmorillonite demonstrated that the Ga had been pillared successfully. As the Ga is intercalated into the structure the layers of the montmorillonite are propped apart,

and the basal spacing (the d-spacing along the c-axis, or 001 reflection) increases from about 14Å to 19.9Å (Figure 2). After calcination at 450°C the d_{001} spacing reduced to 17.9Å. The clean pattern of the intercalated clay indicated that the intercalation process had completed and that no non-pillared montmorillonite remained in the sample.

Figure 3a shows the laminar structure of a single grain of $Al_{12}Ga$ pillared montmorillonite, prepared by simple deposition from suspension onto a TEM grid. Figures 3b-d are high magnification TEM images of resin embedded sections of the Ga_{13}, $Al_{12}Ga$ and Al_{13} pillared montmorillonites, together with electron diffraction patterns showing the (001) diffraction spots. The images also show detailed views of lattice fringes and corresponding spacings in specific areas. The observed lattice fringe spacings from TEM of the pillared clays ranged from 12.9 to 18.2 Å, with a mean value of about 15.2 Å. However, it is clear from the micrographs that the fringe spacings can vary quite considerably, particularly where there is pronounced curvature of the crystals (Figure 3c, arrow). Two different fringe spacings can be observed in the detailed view in Figure 3d. This variability should be reflected in some broadening of the (001) peak in the XRD pattern and this is what is observed (Figure 1). There is some suggestion that the layers are more clearly defined in the $Al_{12}Ga$ pillared montmorillonite, and this may be due to the fact that the central Ga^{IV} atom fits much better in the Keggin-type complex, thereby not only increasing the thermal stability [9], but also the stability of the pillared clay under the electron beam in the TEM. We did observe a noticeable loss of structure in these materials due to beam damage after a short period of TEM viewing, especially at high magnifications.

Measurements of the (001) spacing from electron diffraction patterns of cross-sections of the pillared clays gave a mean value of 15.6 Å (range 14.4 – 17.4 Å), which is consistent with the spacings observed in the micrographs. The patterns also showed fine arcs at 4.45 Å, corresponding to (100) reflections, and in one case spots at 2.29 Å, probably (113) reflections from an adjacent crystal. Overall, the electron diffraction patterns were most consistent with the Montmorillonite-15A structure for a Wyoming montmorillonite (ICDD powder diffraction database #29-1498), for which d_{001}, d_{100} and d_{113} are 15.542, 4.473 and 2.311 Å respectively. However both the observed lattice spacings in the micrographs and the measured (001) spacings from the electron diffraction patterns are on average lower than the basal spacing of 17.9 Å measured by XRD for the Ga_{13} pillared clay. This difference may arise from the different preparation methods used. The XRD measurements were made on powdered material in ambient air, while the TEM measurements were made from thin sections of resin-embedded clay in a high vacuum. The TEM preparation required extensive drying of the clay samples prior to resin embedding and polymerisation and this may explain the differences observed.

Figure 4 shows an X-ray intensity map for Al, Si and Ga in a thin cross-section of a single grain of the Ga_{13} pillared clay. The map demonstrates that the distribution of Ga is closely related to that of Al and Si, and that Ga is present throughout the grain thickness. The estimated electron probe diameter in STEM mode under the conditions used was about 4 nm, consequently there is insufficient spatial resolution to distinguish the layers directly. To measure the amount of Ga in the Ga_{13} pillared clay, eight EDX analyses were

taken from individual small grains or very small clusters of grains. Ga was present in all these spectra in roughly equivalent amounts. The other pillared clays were analysed in a similar manner. EDX spectra from the three pillared clays, compared in each case with a spectrum from the starting montmorillonite, are shown in Figure 5. The Ga K and L X-ray lines are clearly discernible even in the $Al_{12}Ga$ pillared material, and excess Al is evident in the clays pillared with Al_{13} and $Al_{12}Ga$. Both atomic ratios to silicon and concentrations of the elements were calculated from the spectra. The ratio to Si was used since Si is a relatively constant element within the structure and is not affected by the pillaring process. The mean concentrations from EDX analyses of the three pillared clays as well as from the starting materials are listed in Table 1, and do show some variation between the different pillared and starting clays analysed.

From the spectra, the mean atomic ratio of Ga to Si was 0.024 ± 0.001 (SD, n = 10) for the $Al_{12}Ga$ pillared clay, and 0.235 ± 0.015 (SD, n = 8) for the Ga_{13} pillared clay. The ratio of total Al/Si was 0.646 in the Al_{13} pillared material, as compared to a mean of 0.373 in the Miles starting clay, therefore the overall Al_{13}/Si ratio was 0.273. For the $Al_{12}Ga$ pillared material, the total (Al+Ga)/Si ratio was 0.608, which gives an overall $Al_{12}Ga$/Si ratio of 0.235 after allowing for the Al in the starting material. Thus the ratios of pillared element to Si were 0.273, 0.235 and 0.235 respectively in the three pillared clays, suggesting that a roughly constant proportion of the pillared element is incorporated into the structure.

A more reliable correction for the Al content in the tetrahedral and octahedral layers is obtained by calculating the stoichiometric formula of the clay. This has been done in Table 1 for the analysed clays using the mean element concentration data from the X-ray microanalyses. The analyses were calculated into a chemical formula based on a net negative charge of 44 (20 oxygen atoms + 4 hydroxyls). The calculated formula reflects the chemical analysis of SWy-2 montmorillonite well and is very close to the composition described for this CMS source clay [21]. For the Ga_{13} pillared clay, the formula indicates an average of 0.89 Ga atoms per structural unit.

From the information above obtained by EDX analysis and the structure of the montmorillonite, it is possible to calculate the size of the Ga pillars in the Ga_{13} pillared clay. From the literature the thickness of a single clay layer (consisting of one octahedral sheet sandwiched between two tetrahedral sheets) is about 9.8 Å. A basal spacing for the Ga pillared clay of 18.5 Å then results in a height of the Ga pillars of around 8.7 Å, which is close to the value of 9.8 Å for the hydrated complex in solution taking into account the decrease in size during the calcination in which the complex looses all its water and hydroxyl groups [22, 23]. The formula calculated from the EDX analyses shows 0.89 Ga per unit formula, which contains about 8 (Si+Al). There are 6 tetrahedra needed to form a silicate ring, so a total of 19.45 rings are needed to accommodate one Ga_{13} pillar. If we consider a total number of 20 silicate rings per pillar this will result in 10 rings of the top layer and another 10 rings of the bottom layer. From the literature the dimension of the silicate ring is about 5.3 Å [24] so 10 rings correspond to 53 Å. The Ga_{13} shape being a Keggin structure can be considered to be equi dimensional so it is possible to use the height of Ga_{13} as indicated from XRD measurements of the basal spacing for the size of

the pillar. Then the actual dimension of the pillars is 8.7 Å and the distance between the pillars is 53Å – 8.7Å = 44.3Å. The N_2 adsorption-desorption measurements show a quite homogeneous pore size distribution with an average pore size of 39 Å (Figure 6), and the value of 44.3 Å calculated above is in very good agreement with this mean pore size. This calculation is based on average dimensions and it is clear from the TEM images and electron diffraction measurements that the basal spacing does vary within the structure, so it would be expected that the actual distribution of the pillars within the interlayer space may not be homogeneous, but may be analogous to that found for Zr pillars by Crozier *et al.* [18].

4. Conclusions

Wyoming SWy-2 montmorillonite has been used to produce Ga_{13} pillared clay with a mean basal spacing of about 17.9Å, as determined by XRD. This material was prepared for analysis by TEM by orienting the clay particles, embedding them in Spurrs resin, and then ultramicrotoming to produce cross-sections of the clay grains. For comparison Al_{13} and $Al_{12}Ga$ pillared montmorillonites were prepared in a similar manner. Ga_{13} pillared montmorillonite appears to have a similar structure to the Al_{13} and $Al_{12}Ga$ pillared materials, but has the advantage that the Ga incorporated in the clay can be easily analysed by energy-dispersive X-ray microanalysis without confusion with the Al in the structure. Detailed X-ray maps of Ga, Si and Al in cross-sections of the clay grains showed a good correlation between the three elements and also indicated that the Ga was present throughout the structure. Direct measurements of basal layer spacings from TEM micrographs, as well as determinations of spacings from electron diffraction patterns, gave layer spacings that were about 10% lower than the values expected from XRD measurements. However this difference may have been mainly due to the drying, resin embedding and polymerisation used for processing the specimens for TEM.

By allowing for the average amount of Al in the structure of the starting clay material, it is estimated from the EDX microanalyses of the three clays that an approximately constant amount of the intercalated elements is incorporated into the montmorillonite structure. The estimated atomic fractions of the total intercalated species to silicon were 0.273, 0.235 and 0.235 for the Al_{13}, $Al_{12}Ga$ and Ga_{13} pillared clays respectively. By detailed calculation of the clay stoichiometries from the EDX data, it was shown that 0.89 Ga atoms are present per formula unit, which indicates that there are 20 silicate rings consisting of 6 tetrahedral each per Ga_{13} pillar. Thus the average distance between the pillars has been calculated to be 44 Å. This value is close to the average pore size of 39 Å that was determined from N_2 adsorption-desorption measurements of the pillared clay. As the ratio of $Al_{12}Ga$ to Si was similar to that for Ga_{13}/Si, we expect that the distribution of $Al_{12}Ga$ pillars is similar to that of Ga_{13}. The ratio Al_{13}/Si was somewhat higher than for $Al_{12}Ga$ and Ga_{13}, hence the average distance between the Al_{13} pillars should be somewhat less than the 44 Å estimated for the Ga_{13}.

The information from microanalyses in the TEM, in combination with data from XRD and N_2 adsorption-desorption measurements, has allowed us to determine some fundamental information about the distribution of the pillars in the pillared clay. The finding that nearly one pillared atom is incorporated per structural unit in the clay

suggests that a specific bonding site may be involved in the pillaring process within the interlayer. Further details of the pillaring mechanism are currently being investigated using other techniques.

ACKNOWLEDGEMENTS
We wish to thank Mr Tony Raftery for his expert assistance with the XRD measurements, and members of the clay group in the Inorganic Materials Research Program for helpful advice and discussion. We acknowledge financial support from the Inorganic Materials Research Program, Faculty of Science, Queensland University of Technology.

REFERENCES
[1. J. T. Kloprogge, J. Porous Mater. 5 (1998) 5.
2. S. M. Bradley, R. A. Kydd and K. K. Brandt, Stud. Surf. Sci. Catal. 73 (1992) 287.
3. S. M. Bradley and R. A. Kydd, J. Catal. 142 (1993) 448.
4. R. T. Yang, J. P. Chen, E. S. Kikkinides, L. S. Cheng and J. E. Cichanowicz, Ind. Eng. Chem. Res. 31 (1992) 1440.
5. A. Vaccari, Catal. Today 41 (1998) 53.
6. T. J. Pinnavaia, NATO ASI Ser., Ser. C 165 (1986) 151.
7. F. Figueras, Catal. Rev. - Sci. Eng. 30 (1988) 457.
8. W. Jones, Catal. Today 2 (1988) 357.
9. S. M. Bradley, R. A. Kydd, R. Yamdagni and C. A. Fyfe, Synth. Microporous Mater. (1992) 13.
10. S. M. Bradley, R. A. Kydd and R. Yamdagni, Magn. Reson. Chem. 28 (1990) 746.
11. S. M. Bradley, R. A. Kydd and R. Yamdagni, J. Chem. Soc., Dalton Trans. (1990) 2653.
12. A. Bellaloui, D. Plee and P. Meriaudeau, Appl. Catal. 63 (1990) L7.
13. A. V. Coelho and P. G., Appl. Catalysis 77 (1991) 303.
14. F. Gonzalez, P. C., B. I. and M. S., J. Chem. Soc. (1991) Chem. Commun.
15. E. Montarges, L. J. Michot and P. Ildefonse, Microporous and Mesoporous Mater. 28 (1999) 83.
16. J.-W. Kim, D. R. Peacor, D. Tessier and F. Elsass, Clays Clay Miner. 43 (1995) 51.
17. C. Ma, D. Fitzgerald, R. A. Eggleton and D. J. Llewellyn, Clays Clay Miner. 46 (1998) 301.
18. P. A. Crozier, M. Pan, C. Bateman, J. J. Alcaraz and J. S. Holmgren, Clays Clay Miner. 47 (1999) 683.
19. J. T. Kloprogge, R. Evans, L. Hickey and R. L. Frost, Appl. Clay Sci. 20 (2002) 157.
20. A. R. Spurr, Journal of Ultrastructural Research 26 (1969) 31–43.
21. A. R. Mermut and A. F. Cano, Clays Clay Miner. 49 (2001) 381.
22. M. L. Occelli, A. Auroux and G. J. Ray, Microporous Mesoporous Mater. 39 (2000) 43.

23. M. L. Occelli, J. A. Bertrand, S. A. C. Gould and J. M. Dominguez, Microporous Mesoporous Mater. 34 (2000) 195.
24. W. A. Deer, R. A. Howie and J. Zussman, An introduction to the Rock-Forming Minerals, 2nd ed., Addison Wesley Longman Ltd., Harlow, 1996.

Figure Captions

Figure 1. Preparation of cross sections of a clay sample for TEM.

Figure 2. XRD patterns of a) starting Wyoming Swy2 montmorillonite, b) montmorillonite exchanged with Ga_{13} showing an interlayer spacing of 19.9 Å, and c) Ga_{13} pillared montmorillonite with a spacing oft 17.9 Å.

Figure 3. TEM image of a) a grain of $Al_{12}Ga$ pillared montmorillonite; and images and electron diffraction patterns from sectioned material: b) Ga_{13} pillared montmorillonite; c) $Al_{12}Ga$ pillared montmorillonite and d) Al_{13} pillared montmorillonite.

Figure 4. Elemental X-ray maps for Ga, Si and Al from a cross section of a single grain of Ga_{13} pillared montmorillonite.

Figure 5. EDX spectra from analyses in the TEM of small grains of (a) Ga_{13} pillared, (b) $Al_{12}Ga$ pillared, and (c) Al_{13} pillared montmorillonites. The spectra are shown overlaid with a spectrum from the starting material. The C and Cu peaks derive from the resin or thin carbon coating and the TEM grid material respectively.

Figure 6. Pore size distribution of Ga_{13} pillared montmorillonite.

Table 1. Characteristic concentrations (single analysis) in weight % from X-ray microanalyses in the TEM of the starting and the Ga_{13}-, $Al_{12}Ga$- and Al_{13}-pillared montmorillonites (top), and the formula calculation based on 22 oxygens (bottom).

Element	Starting Mont. (Swy-2)	Starting Miles Mont.	Ga_{13} Pilc Swy-2	Al_{13}-Pilc Miles	$Al_{12}Ga$-Pilc Miles
Na	1.23	2.15	0	0	0.20
Mg	1.49	1.71	0.3	1.21	1.07
Al	10.68	9.86	10.00	13.87	13.82
Si	27.12	26.66	25.15	25.85	29.41
K	0.06	0.22	0.02	0	0.03
Ca	0.09	0.64	0.15	0	0.09
Ti	0.10	0.05	0	0.25	0.18
Fe	2.78	2.39	2.55	2.26	2.88
Ga	0	0	2.85	0	0.72

Calculated formula based on 22 oxygens	
Starting montmorillonite Swy-2	$(Na_{0.14}K_{0.08}Ca_{0.04})(Mg_{0.49}Fe^{3+}_{0.40}Ti_{0.04}Al_{3.09})(Si_{7.87}Al_{0.13})O_{20}(OH)_4.nH_2O$
Ga_{13} pillared montmorillonite	$Ga_{0.89}(Mg_{0.60}Fe^{3+}_{0.21}Ti_{0.02}Al_{3.09})(Si_{7.87}Al_{0.13})O_{20}(OH)_4.nH_2O$
Starting Miles montmorillonite	$(Na_{0.95}K_{0.02}Ca_{0.084})(Mg_{0.60}Fe^{3+}_{0.12}Ti_{0.005}Al_{3.11})(Si_{7.95}Al_{0.05})O_{20}(OH)_4.nH_2O$
Al_{13} pillared montmorillonite	$Al_{1.46}(Mg_{0.65}Fe^{3+}_{0.18}Ti_{0.010}Al_{3.11})(Si_{7.95}Al_{0.05})O_{20}(OH)_4.nH_2O$
$Al_{12}Ga$ pillared montmorillonite	$Al_{2.28}Ga_{0.19}(Mg_{0.40}Fe^{3+}_{0.78}Ti_{0.017}Al_{0.91})(Si_{7.95}Al_{0.05})O_{20}(OH)_4.nH_2O$

Table 1

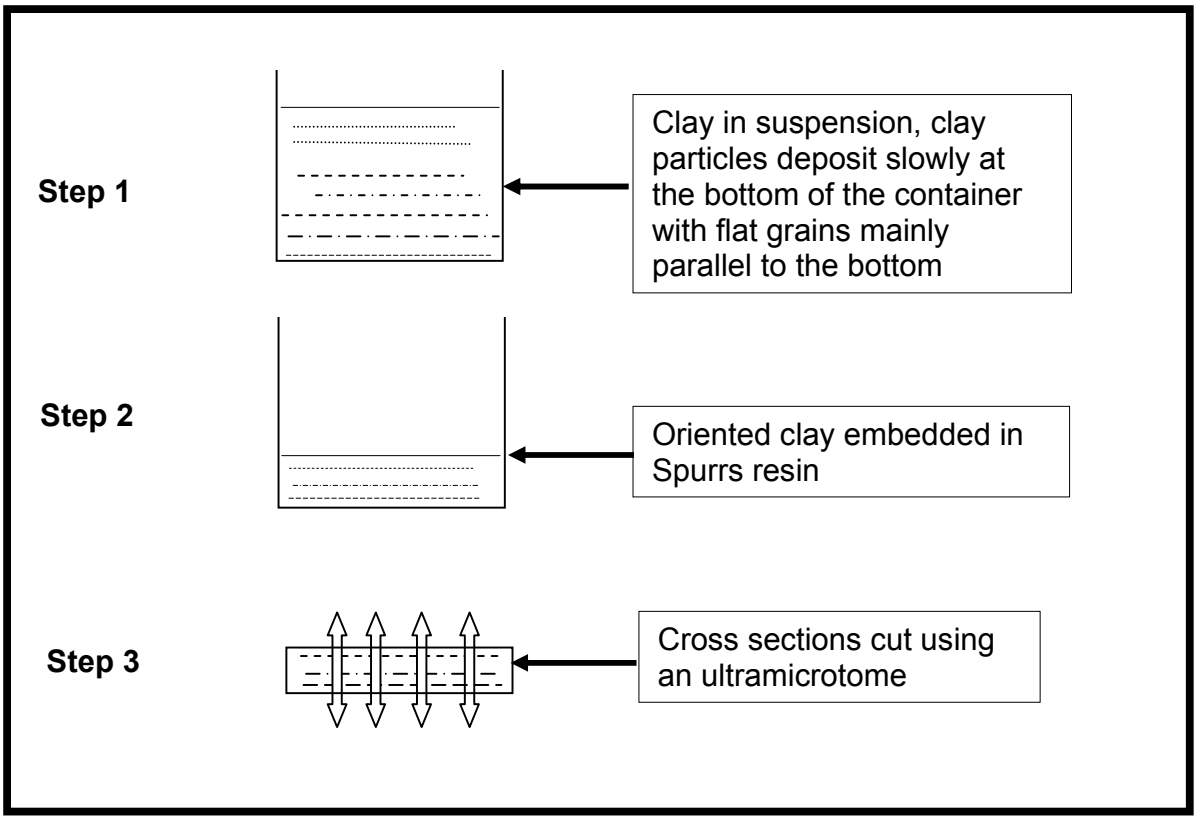
Step 1
Clay in suspension, clay particles deposit slowly at the bottom of the container with flat grains mainly parallel to the bottom
Step 2
Oriented clay embedded in Spurrs resin
Step 3
Cross sections cut using an ultramicrotome

Figure 1

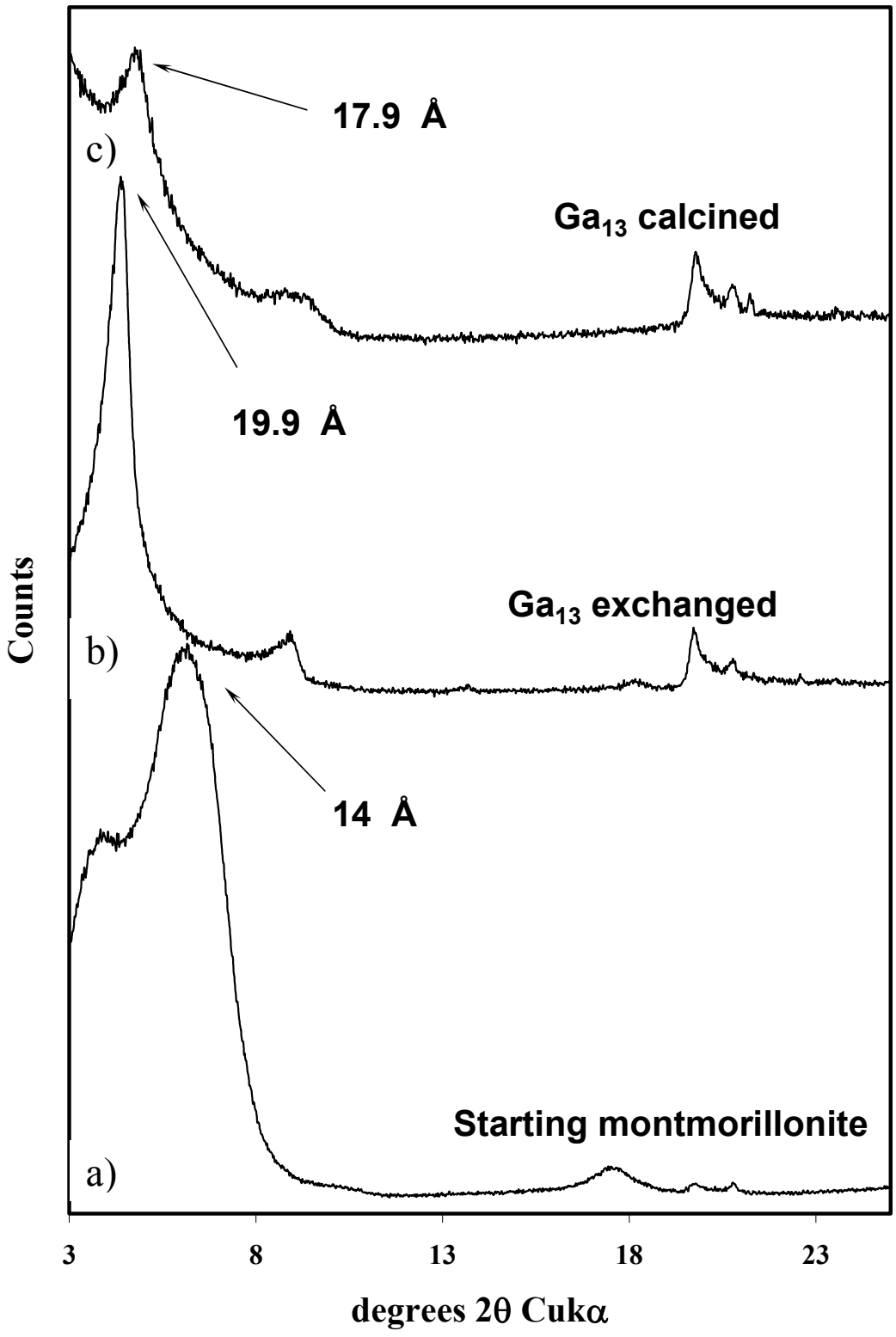
17.9 Å
c)
Ga13 calcined
19.9 Å
Ga13 exchanged
b)
14 Å
Starting montmorillonite
a)
Counts
3
8
13
18
23
degrees 2θ Cukα

Figure 2

FIGURE 3

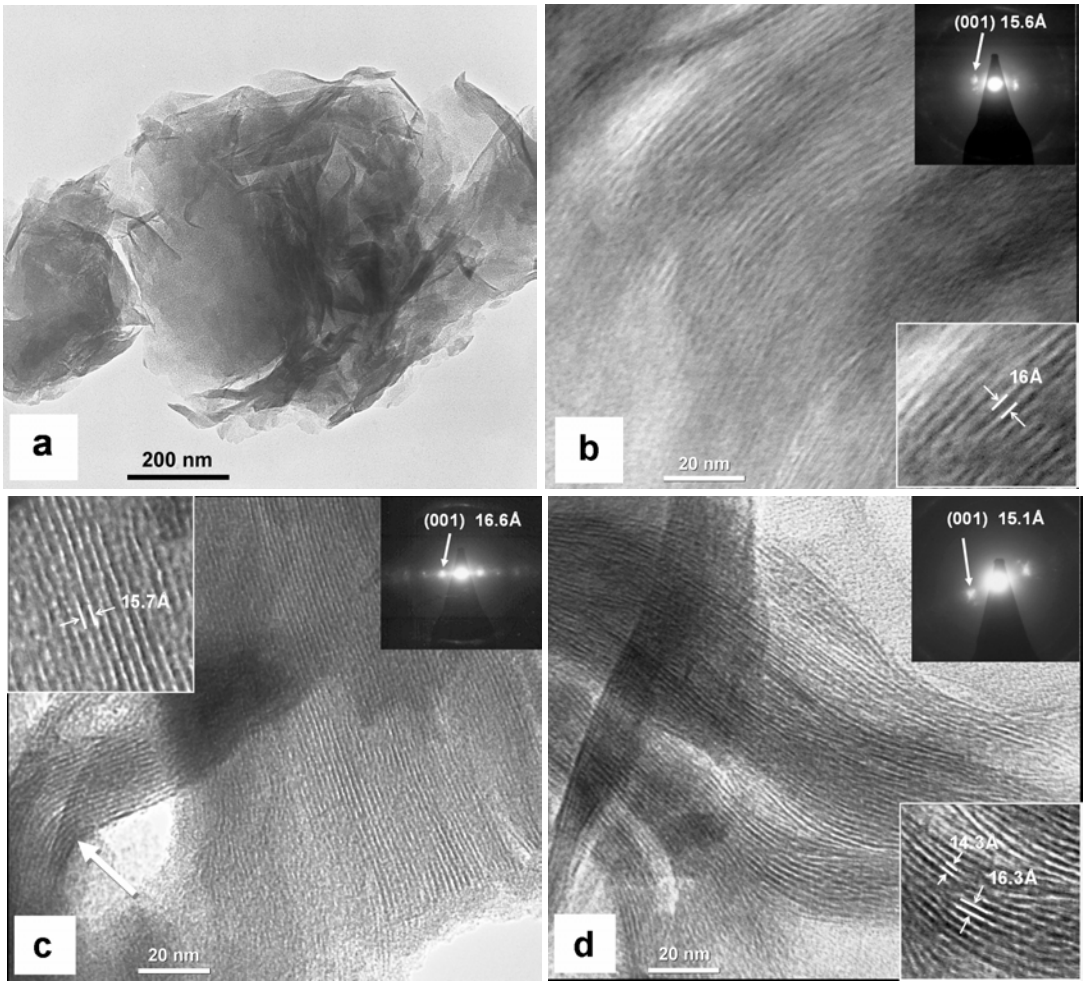
a
200 nm
b
(001) 15.6Å
16Å
20 nm
c
(001) 16.6Å
15.7Å
20 nm
d
(001) 15.1Å
14.3Å
16.3Å
20 nm

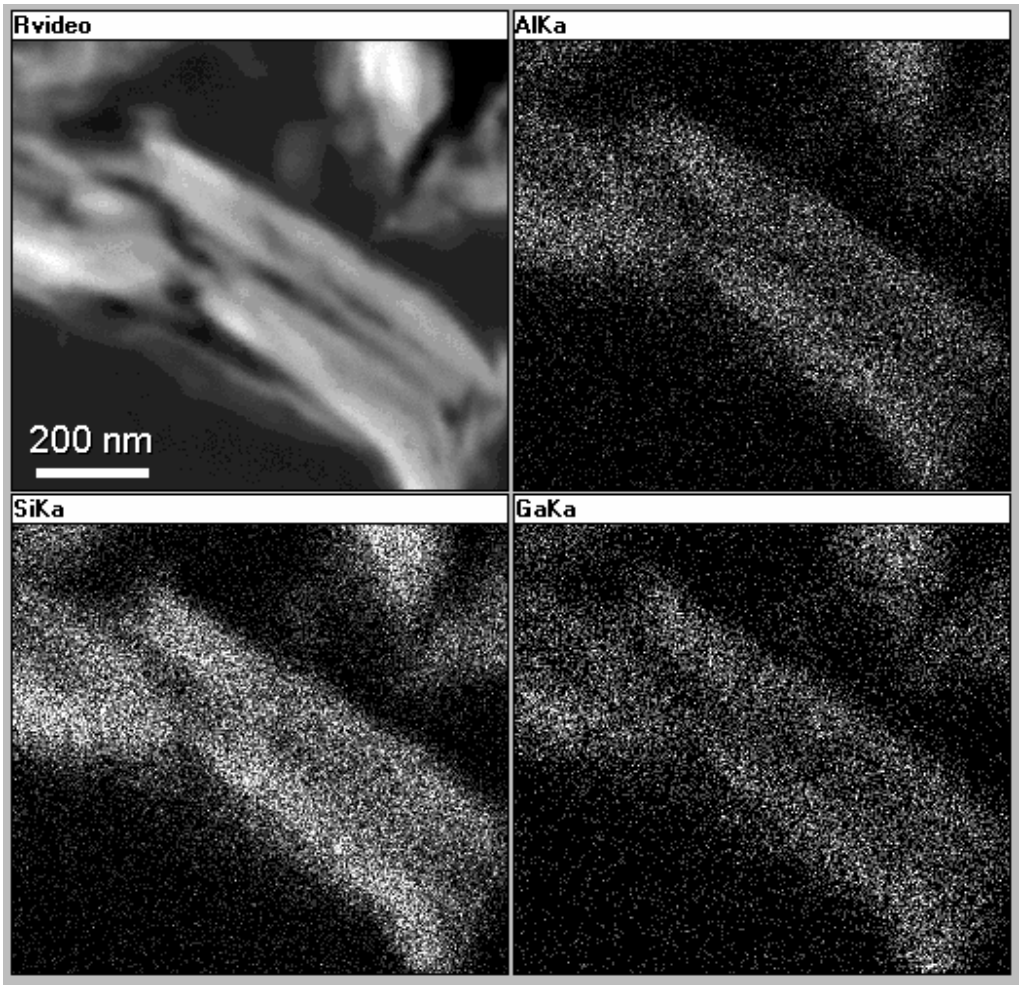

Figure 4

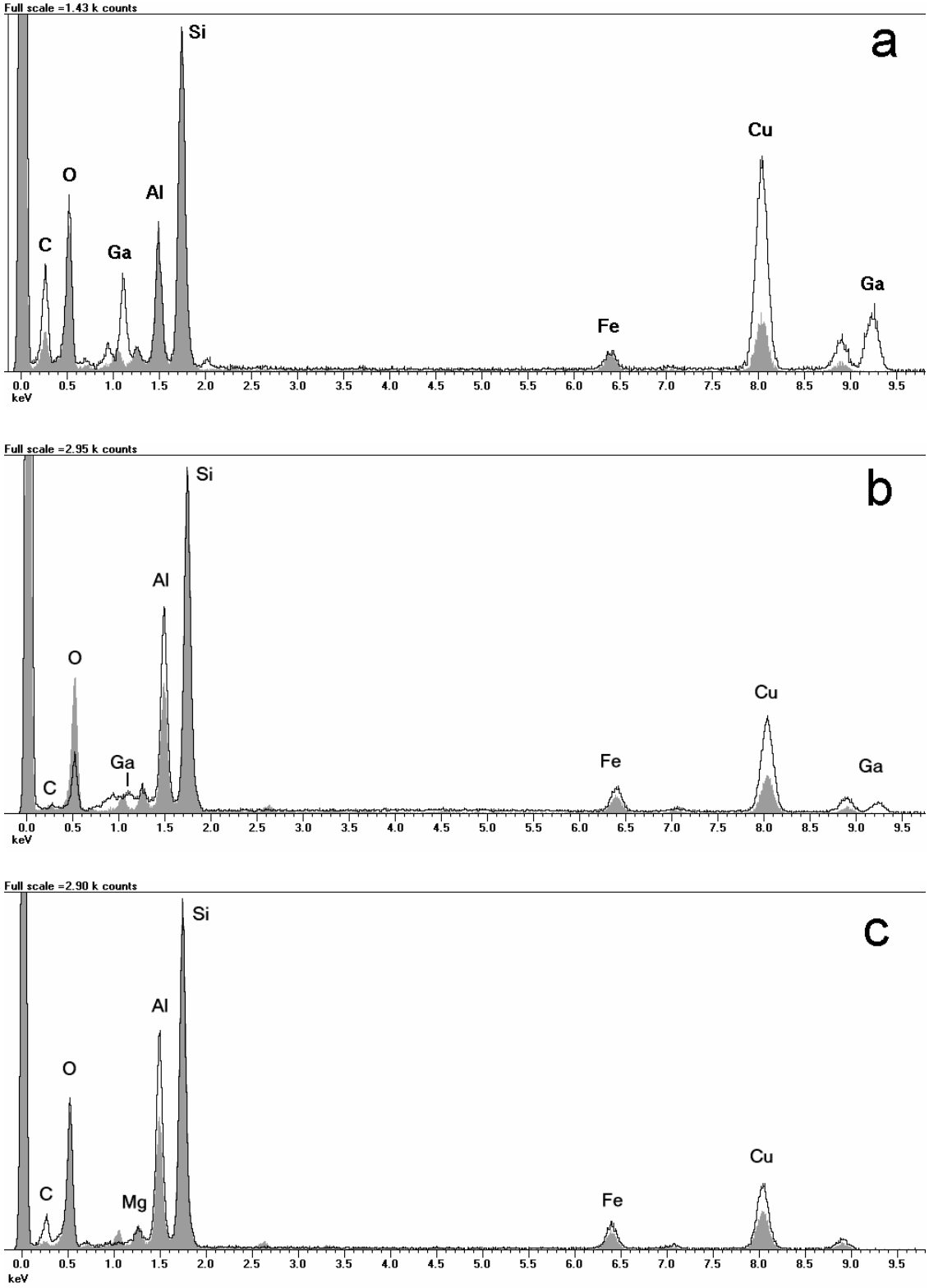
Full scale =1.43 k counts
a
Si
O
Al
C
Ga
Cu
Ga
Fe
0.0 0.5 1.0 1.5 2.0 2.5 3.0 3.5 4.0 4.5 5.0 5.5 6.0 6.5 7.0 7.5 8.0 8.5 9.0 9.5
keV
Full scale =2.95 k counts
b
Si
Al
O
Cu
Ga
C
Fe
Ga
0.0 0.5 1.0 1.5 2.0 2.5 3.0 3.5 4.0 4.5 5.0 5.5 6.0 6.5 7.0 7.5 8.0 8.5 9.0 9.5
keV
Full scale =2.90 k counts
c
Si
Al
O
Cu
C
Mg
Fe
0.0 0.5 1.0 1.5 2.0 2.5 3.0 3.5 4.0 4.5 5.0 5.5 6.0 6.5 7.0 7.5 8.0 8.5 9.0 9.5
keV

Figure 5

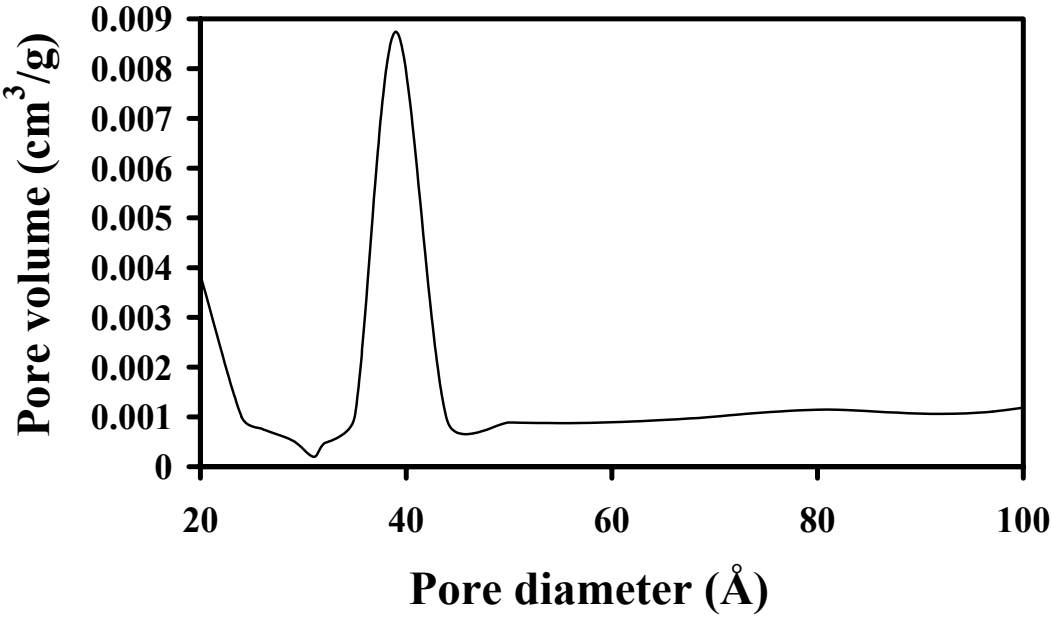
Pore volume (cm3/g)
0.009
0.008
0.007
0.006
0.005
0.004
0.003
0.002
0.001
0
20
40
60
80
100
Pore diameter (Å)

Figure 6